Thermal conductivity of GaN films: Effects of impurities and dislocations

J. Zou, D. Kotchetkov, and A. A. Balandin[a)]
Department of Electrical Engineering, University of California at Riverside, Riverside, California 92521

D. I. Florescu[b)] and Fred H. Pollak
Physics Department and New York State Center for Advanced Technology in Ultrafast Photonic Materials and Applications, Brooklyn College of the City University of New York, Brooklyn, New York 11210

(Received 6 March 2002; accepted for publication 5 June 2002)

We report details of the calculation of the lattice thermal conductivity κ in wurtzite GaN. Numerical simulations are performed for *n*-type wurtzite GaN with different density of silicon dopants, point defects and threading dislocations. Using the material specific model we verified the experimentally observed linear decrease of the room-temperature thermal conductivity with the logarithm of the carrier density n. The decrease was attributed mostly to the increased phonon relaxation on dopants. Our calculations show that the increase in the doping density from 10^{17} to 10^{18} cm^{-3} leads to about a factor of 2 decrease in thermal conductivity from 1.77 W/cm K to 0.86 W/cm K. We have also established that the room-temperature thermal conductivity in GaN can be limited by dislocations when their density is high, e.g., $N_D > 10^{10}$ cm^{-2}. The obtained results are in good agreement with experimental data. The developed calculation procedure can be used for accurate simulation of self-heating effects in GaN-based devices. © *2002 American Institute of Physics.*
[DOI: 10.1063/1.1497704]

I. INTRODUCTION

Proposed applications of GaN-based devices as laser diodes, microwave power sources and ultrahigh power switches rely heavily on the possibility of removing high density of excess heat from the device active area. Self-heating strongly affects the performance of high-power AlGaN/GaN heterostructure field-effect transistors and rf devices.[1,2] Different methods of effective heat dissipation, such as flip-chip bonding or substrate removal, have been envisioned for GaN-based devices.[3] The material of an active layer and the substrate material generally determine the thermal resistance of the device structure. Thus, it is important to know the accurate values of the thermal conductivity of corresponding materials and their dependence on doping densities and dislocation concentration in order to perform heat spreading simulations and obtain thermal constrains on the device design.

The first measurements of the thermal conductivity κ of GaN films grown by hydride vapor phase epitaxy revealed a rather low value of about 1.3 W/cm K at room temperature.[4] More recently, using the scanning thermal microscopy technique, Florescu *et al.*[5] determined that the thermal conductivity of the GaN films fabricated by the lateral epitaxial overgrowth (LEO) is about 1.7–1.8 W/cm K. For some samples the thermal conductivity value reaches $\kappa=2.1$ W/cm K on the stripe regions characterized by lower dislocation density. The latter value is much higher than that in between stripes, e.g., in the vicinity of the SiN_x mask, where the density of dislocations and impurities is very high. Florescu *et al.*[6] have also reported the thermal conductivity measurements at room temperature on GaN/sapphire (0001) samples fabricated by hybrid vapor phase epitaxy (HVPE). In this work thermal conductivity was measured as a function of carrier concentration. For all sets of examined samples, it was found that thermal conductivity decreases linearly with log n: about a factor of 2 decrease in κ for every decade increase in the carrier density n. One should mention here that the observed decrease is most likely not due to increased phonon-carrier scattering but rather due to the increased scattering of phonons on dopants. Another group has also reported the room-temperature thermal conductivity of LEO GaN films to be in excess of $\kappa=1.55$ W/cm K.[7]

In our recent letter[8] we have demonstrated that the discrepancy between early GaN thermal conductivity data[4] and new results obtained for LEO[5,7] and HVPE[6] samples can be attributed to phonon scattering on dislocations and point defects. Moreover, we were able to correlate the experimentally observed difference in the thermal conductivity values for the stripe and seam lines in LEO samples with the difference in the dislocation density in the stripe and seam regions.[8] In this paper we report details of our calculation and examine the effects of doping and impurities on the thermal conductivity. At the end we compare our numerical results with experimental data for κ dependence on carrier concentration reported in Ref. 6.

The rest of the paper is organized as follows. In the next section we present details of the theoretical model where we include scattering mechanisms specific for GaN. In Sec. III we describe impurities characteristic for GaN, provide numerical results for the thermal conductivity and compare them with experimental data. Conclusions are given in Sec. IV.

[a)]Author to whom correspondence should be addressed; electronic mail: alexb@ee.ucr.edu
[b)]Present address: Emcore Corporation, 145 Belmont Drive, Somerset, NJ 08873.

Downloaded 19 Aug 2002 to 138.23.167.22. Redistribution subject to AIP license or copyright, see http://ojps.aip.org/japo/japcr.jsp

II. MODEL

Among known possible crystal structures for the group-III nitrides, the thermodynamically stable one under ambient conditions is wurtzite (hexagonal) structure. In wurtzite GaN, to which we restrict our analysis, the lattice constants at room temperature are $a=3.189$ Å and $c=5.185$ Å. One should note here that *we do not use fitting parameters* in our simulation. Instead, we calculate thermal conductivity for different sets of material parameters reported for GaN in literature. The calculation is based on the phonon relaxation rates found from the perturbation theory. Our simulation results are then compared with available experimental thermal conductivity data.

A. Lattice thermal conductivity

In technologically important semiconductors, the dominant contribution to the room-temperature thermal conductivity comes from acoustic phonons.[9] Florescu *et al.*[6] experimentally determined that the electronic contribution to thermal conductivity in GaN is about $\kappa_e \sim 1.5\times 10^{-3}$ W/cm K which is *three orders* of magnitude smaller than the typical value of the lattice thermal conductivity. Thus, here we neglect the electronic contribution to thermal conductivity. We base our calculations on Callaway's phenomenological theory[10] and Klemens' second-order perturbation theory formulas for phonon scattering rates.[11] In Callaway's formulation the lattice thermal conductivity involves two terms $\kappa = \kappa_1 + \kappa_2$, where κ_1 and κ_2 are given by

$$\kappa_1 = \left(\frac{k_B}{\hbar}\right)^3 \frac{k_B}{2\pi^2 v} T^3 \int_0^{\theta_D/T} \frac{\tau_C x^4 e^x}{(e^x-1)^2} dx, \tag{1}$$

$$\kappa_2 = \left(\frac{k_B}{\hbar}\right)^3 \frac{k_B}{2\pi^2 v} T^3 \frac{\left\{\int_0^{\theta_D/T} (\tau_C/\tau_N) x^4 e^x (e^x-1)^{-2} dx\right\}^2}{\int_0^{\theta_D/T} \tau_C/(\tau_N\tau_R)\} x^4 e^x (e^x-1)^{-2} dx}. \tag{2}$$

Here, k_B is the Boltzmann's constant, $\hbar$ is the Plank constant, T is absolute temperature, v is an average sound velocity, $\tau_N \equiv \tau_N(x) [\tau_R \equiv \tau_R(x)]$ is relaxation time in normal (resistive) processes, $\tau_C \equiv \tau_C(x)$ is combined relaxation time, ω is the phonon frequency, and $x = \hbar\omega/k_B T$. This model assumes Debye-like phonon density of states, one effective acoustic-phonon dispersion branch, and the additivity of the relaxation rates for independent scattering processes, so that $\tau_C^{-1} = \tau_R^{-1} + \tau_N^{-1}$. Here τ_R includes relaxation in three-phonon Umklapp processes, point defects, and dislocations. The relaxation rates in normal processes become comparable to those in resistive processes ($\tau_N \approx \tau R$) only in very pure, defect-free samples. In GaN films the concentration of static imperfections (point defects, vacancies, dislocations, etc.) is very high which leads to the total dominance of resistive processes and the condition $\tau_N >> \tau_R$ so that $\tau_C \approx \tau_R$ and $\kappa \approx \kappa_1$.

In real crystals, the sound velocity v (**q**) depends on the direction and magnitude of the phonon wave vector **q**, and is specific to a given phonon polarization type. In the spirit of Callaway's formulation, we use a single-branch polarization-averaged velocity v along a specified crystallographic direction

TABLE I. Material parameters in GaN.

Material parameters		Set I	Set II
Lattice constant	a (Å)	3.189[a]	3.189[a]
Lattice constant	c (Å)	5.185[a]	5.185[a]
Volume per atom	V_0 (Å^3)	11.42	11.42
Gruneisen parameter	γ	0.74[b]	0.74[b]
Density	ρ (kg/m^3)	6150[a]	6150[a]
Longitudinal elastic constant	C_L (GPa)	265	398
Transverse elastic constant	C_T (GPa)	44.2	105
Shear modulus	μ (GPa)	44.2	105
Longitudinal sound velocity	v_L (m/s)	6560	8040
Transverse sound velocity	v_T (m/s)	2680	4130
Polarization averaged velocity	v (m/s)	3338	4929
Debye temperature	θ_D (K)	1058[a]	1058[a]

[a]From Ref. 12.
[b]From Ref. 23.

$$v = \left[\frac{1}{3}\left(\frac{1}{v_{T,1}} + \frac{1}{v_{T,2}} + \frac{1}{v_L}\right)\right]^{-1}, \tag{3}$$

where v_L and $v_{T,1,2}$ are the longitudinal and transverse sound velocities, respectively. Along [001] direction, which corresponds to [0001] four-axes notation used for hexagonal lattice, two transverse branches are degenerate and have the same velocity given by $v_{T,1} = v_{T,2} = v_T = (C_{44}/\rho)^{1/2}$; the longitudinal velocity is defined as $v_L = (C_{33}/\rho)^{1/2}$. Along [100] direction, two transverse polarizations have different velocities given by $v_T = (C_{44}/\rho)^{1/2}$ and $v_T = [(C_{11} - C_{12})/\rho]^{1/2}$. Here, $C_{i,j}$ are the elastic constants of the crystal. Material parameters extracted from Ref. 12 and Ref. 14 are summarized in Table I. In cases, when dislocation lines and heat flux are considered to be strictly oriented and mutual orientation of dislocation lines and a temperature gradient are important, one can use general formulas for the sound velocity given by Deguchi *et al.*[13]

B. Phonon relaxation rates

In Callaway and Klemens' formulation, the combined relaxation rate can be written as a sum of the resistive scattering probabilities $1/\tau_C \approx 1/\tau_R = \Sigma_i 1/\tau_i$, where τ_i represents relaxation times relevant to a given material system. For GaN the important relaxation processes are Umklapp scattering (τ_U), point defect (impurity atoms and vacancies only) scattering (τ_P), and scattering on dislocations (τ_D). We do not include isotope and boundary scattering rates since they are important for extremely pure samples or at very low temperature. From the second-order perturbation theory, the relaxation time for three-phonon Umklapp scattering at high temperature ($T=300$ K and above) is given by[15]

$$\frac{1}{\tau_U} = 2\gamma^2 \frac{k_B T}{\mu V_0} \frac{\omega^2}{\omega_D}, \tag{4}$$

where γ is the Gruneisen anharmonicity parameter, μ is the shear modulus, V_0 is the volume per atom, and ω_D is the Debye frequency. The shear modulus μ in Eq. (4) is related

Downloaded 19 Aug 2002 to 138.23.167.22. Redistribution subject to AIP license or copyright, see http://ojps.aip.org/japo/japcr.jsp

to the transverse sound velocity through $\mu = v_T^2 \cdot \rho$. The unit volume V_0 for wurtzite GaN is given by $V_0 = \sqrt{3} a^2 c/8$.[16]

The phonon relaxation on point defects can be written as[11]

$$\frac{1}{\tau_P} = \frac{V_0 \Gamma \omega^4}{4 \pi v^3}, \tag{5}$$

where Γ is the measure of the strength of the point defect scattering. In our letter[8] we assumed for simplicity that the point defect scattering is only due to the difference in mass of substitutional foreign atoms. Here we retain a second term given in the original Klemens' formulation,[17] which is due to scattering of phonons by an elastic strain field of a point defect. The mass of an impurity atom is well known, but the local displacement in the host lattice ΔR $(= \bar{R} - R_i)$ is usually not. Following Ref. 17 we estimate ΔR by assuming that the interionic distances are the sum of the ionic radii, so that the value of ΔR is the difference between the radii of the impurity R_i and host ions. Thus, the strength of the point defect scattering is given by[17,18]

$$\Gamma = \sum_i f_i \left[\left(1 - \frac{M_i}{\bar{M}} \right)^2 + 2 \left\{ 6.4 \gamma \left(1 - \frac{R_i}{\bar{R}} \right) \right\}^2 \right]. \tag{6}$$

Here f_i is the fractional concentration of the impurity atoms, M_i is the mass of the ith impurity atom or defect, $\bar{M} = \Sigma_i f_i M_i$ is the average atomic mass, R_i is the Pauling ionic radius of the ith impurity atom or defect, $\bar{R} = \Sigma_i f_i R_i$ is the average radius. Characteristic residual impurities and doping atoms that were used for calculation of the point-defect scattering term are discussed in the next section.

Due to their large lattice mismatch, heteroepitaxy of GaN on sapphire or SiC substrates results in films with typically large threading dislocation density of about 10^8 cm^{-2} – 10^{11} cm^{-2},[19–21] although some special methods allow us to reduce this density down to 10^5 cm^{-2}.[20] Transmission electron microscopy reveals that the dislocations in GaN films are usually aligned along c axis and could belong to one of three types: edge, screw, or mixed. In our calculation we include all three types of dislocations characteristic for GaN.

Phonon can scatter on dislocations via two distinctive mechanisms. The first one is scattering by the elastic strain field of the dislocation lines, which is a long-range interaction. Similar to the three-phonon Umklapp process the interaction of phonons with the strain field of the dislocation lines is mediated by the higher order terms in the potential energy of real crystals. The second mechanism is scattering of phonons on the core of the dislocation lines, which is a short-range interaction modeled similar to mass-difference scattering on point impurities.[17] The phonon scattering rate at the core of the dislocation $(1/\tau_{\mathrm{DC}})$ is proportional to the cube of the phonon frequency and given by[11]

$$\frac{1}{\tau_{\mathrm{DC}}} = \eta N_D \frac{V_0^{4/3}}{v^2} \omega^3, \tag{7}$$

where N_D is the density of the dislocation lines of all types, and η is the weight factor to account for the mutual orientation of the direction of the temperature gradient and the dislocation line. For dislocations perpendicular to the temperature gradient $\eta = 1$, while for those parallel to the gradient $\eta = 0$. If dislocation lines are orientated at random with respect to the temperature gradient, the average value found by integration is $\eta = 0.55$.[17] The phonon scattering rate by the elastic field of the screw $(1/\tau_S)$ and edge $(1/\tau_E)$ dislocations can be written as[11,17]

$$\frac{1}{\tau_S} = \frac{2^{3/2}}{3^{7/2}} \eta N_D^S b_S^2 \gamma^2 \omega, \tag{8}$$

$$\frac{1}{\tau_E} = \frac{2^{3/2}}{3^{7/2}} \eta N_D^E b_E^2 \gamma^2 \omega \left\{ \frac{1}{2} + \frac{1}{24} \left(\frac{1 - 2\nu}{1 - \nu} \right)^2 \left[1 + \sqrt{2} \left(\frac{v_L}{v_T} \right)^2 \right]^2 \right\}, \tag{9}$$

where $\nu = C_{12}/(C_{11} + C_{12})$ is Poisson's ratio, b_S and b_E are magnitudes of Burgers vectors for the screw and edge dislocations correspondingly. In real crystals, the Poisson ratio is anisotropic and does not have a uniquely defined average value. For the purpose of the present work, its value for GaN is taken to be 0.37, which corresponds to the isotropic case. As the characteristic values of Burgers vectors in GaN films we take[19,21]

$$b_S = c[0001] = c \text{ and } b_E = \frac{a[11\bar{2}0]}{3} = \frac{a\sqrt{2}}{3}.$$

The Burgers vector for the mixed dislocation is $b_M = b_S + b_E$.[21] The scattering rate on mixed dislocations $(1/\tau_M)$ is[11,17]

$$\frac{1}{\tau_M} = \frac{2^{3/2}}{3^{7/2}} \eta N_D^M \gamma^2 \omega \left(b_S^2 + b_E^2 \left\{ \frac{1}{2} + \frac{1}{24} \left(\frac{1 - 2\nu}{1 - \nu} \right)^2 \times \left[1 + \sqrt{2} \left(\frac{v_L}{v_T} \right)^2 \right]^2 \right\} \right). \tag{10}$$

Here, N_D^S, N_D^E, and N_D^M are the densities for the screw, edge, and mixed dislocations, respectively, so that the total density of dislocation is $N_D = N_D^S + N_D^E + N_D^M$. Assuming that phonon relaxation on dislocations is an independent process, the combined phonon relaxation rate on dislocations is then calculated as $1/\tau_D = \Sigma_j 1/\tau_j$, where τ_j represents scattering times on the dislocation core (τ_{DC}), on the elastic strain field of edge (τ_E), screw (τ_S) and mixed (τ_M) dislocations. Assuming $1/\tau_C = 1/\tau_U$ and evaluating integrals in Eqs. (1) and (2), one can calculate the *intrinsic* thermal conductivity, e.g., theoretical limit, for GaN film. The intrinsic thermal conductivity is limited by the crystal anharmonicity only, which is included in the model via the three-phonon Umklapp processes [see Eq. (4)]. For $1/\tau_C = 1/\tau_U + 1/\tau_P + 1/\tau_D$, one obtains the extrinsic thermal conductivity that includes all major phonon resistive relaxation processes, namely scattering on impurities (point defects) and dislocations. It is this value that has to be compared with experiment.

III. RESULTS AND DISCUSSION

There is a significant discrepancy in values of material parameters reported for GaN. For the simulation we use materials parameters shown in Table I. In our calculations we do

Downloaded 19 Aug 2002 to 138.23.167.22. Redistribution subject to AIP license or copyright, see http://ojps.aip.org/japo/japcr.jsp

not use any of the material constants as adjusted parameters but rather evaluate κ for distinctively different sets of reported material constants and then compare the results with available experimental data. For the materials constants indicated as Set I and Set II in Table I we obtain the intrinsic lattice thermal conductivity, e.g., theoretical limit, $\kappa=3.36$ and $\kappa=5.40$ W/cm K, respectively. It is important to emphasize that the relatively large difference between these two values of the intrinsic thermal conductivity is entirely due to ambiguity in elastic constants reported for GaN. These values compare well with the "upper bound" value of $\kappa\sim3.2$ W/cm K deduced by Slack for a similar material such as AlN.[22] The numbers are also in agreement with the theoretical thermal conductivity limit $\kappa=4.1$ W/cm K for GaN calculated in Ref. 23. Since GaN films are very far from being defect free and pure, the experimentally measured values of κ in GaN are much smaller than the calculated intrinsic limit. Below we examine how static defects affect the thermal conductivity value.

In order to include point-defect scattering to our simulation [see Eqs. (5) and (6)] we need to use realistic concentration of impurities in GaN films. In his early study,[22] Slack has noted that in wurtzite AlN the common troublesome impurities that limit thermal conductivity are carbon (C), oxygen (O), and silicon (Si). He also pointed out that oxygen enters the AlN lattice and substitutes for N up to very high oxygen concentration. Characteristic residual impurities in GaN grown by metalorganic chemical vapor deposition (MOCVD) and molecular beam epitaxy (MBE) are also C, O, Si as well as hydrogen (H).[24,25] The common source of H is NH_3, which is used in GaN growth process described by the following formula $(CH_3)_3Ga+NH_3\rightarrow GaN+CH_4\uparrow+H_2\uparrow$.[25] It was found that although H_2 is electrically and optically inactive in all semiconductors, atomic hydrogen diffuses rapidly and can form neutral complexes with dopants.[26] Atomic hydrogen can attach to dangling bonds associated with point defects. There is an evidence that H^- ion is often located at the anti-bonding Ga site and can be attached to Si^+ dopants. Silicon plays the role of a shallow donor, which substitutes Ga. In the present model only negative ions of H^- attached to Si^+ are considered. Two other impurities included in the model are carbon and oxygen. The source of O in GaN is usually NH_3 precursor used in MOCVD growth, the residual water vapor in MBE chambers or O impurities leached from the quartz containment vessel often employed in N_2 plasma sources.[25] The source of carbon impurities in GaN is the metalorganic gallium precursor.[26] Finally, the source of Si impurity in LEO grown samples can be diffusion from SiN_x mask in addition to n-type doping with SiH_4 or Si_2H_6. It is known that samples even without intentional n-type doping have Si concentration comparable to C and H. The last type of impurities taken into consideration is Ga vacancies in GaN.[12,27] For each specific impurity we calculate the scattering rate given by Eqs. (5) and (6), and then add them all. Vacancies are considered to be atom-like entities with $M_i = 0$ and $R_i = 0$.

Figure 1 shows the lattice thermal conductivity in wurtzite GaN as a function of temperature for the fixed concentration of impurities. The material parameters used for this figure are taken from Table I (Set I), the impurity profile is from column A of Table II. The dislocation density is equal to $N_D=10^{10}$ cm^{-2} while the concentration of vacancies is taken to be 10^{16} cm^{-3}. Calculating the scattering on point defects, we assumed that the ionic radii for Ga and N are 62 and 171 pm, respectively. The ionic radii of the impurities are presented in Table II.

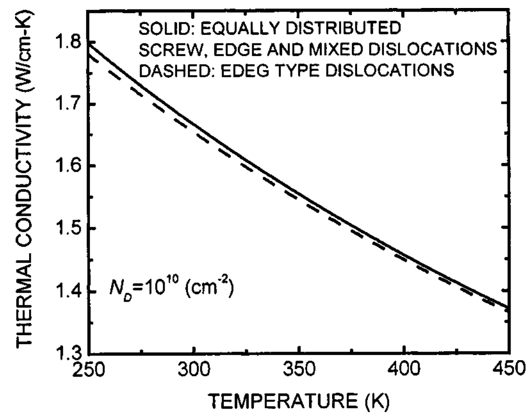

FIG. 1. Thermal conductivity of wurtzite GaN films as a function of temperature. The concentration of threading dislocations is $N_D=10^{10}$ cm^{-2}. The solid curve corresponds to the case when the dislocations are equally distributed among three possible types: screw, edge and mixed. The dashed curve corresponds to the case when all dislocations are of pure edge type. The results are obtained for typical impurity concentrations and phonon velocity averaged over possible polarization branches and directions.

The dashed curve in Fig. 1 corresponds to the case when all threading dislocations are of the edge type. The solid curve is for the case when the dislocations are equally split among three possible types: edge, screw and mixed. According to the transmission electron and x-ray diffraction study reported in Ref. 20 for HVPE grown GaN samples, the assumption of equally distributed dislocations among the possible types is a feasible one. The difference between these two curves is not large because for the chosen value of the dislocation density, Umklapp and point-impurity scattering contribute stronger to the acoustic phonon relaxation than scattering on dislocations. A characteristic $1/T$ dependence seen in this plot is typical for crystalline solids at high temperature and it is due to Umklapp scattering. In calculation we assumed random orientation of dislocations with respect to the heat flux lines so that $\eta=0.55$. This leads to the directionally averaged κ and roughly corresponds to the scanning thermal microscopy measurements where heat is generated by a point source and propagates in all directions.[5,6]

In Figs. 2(a) and 2(b) we present thermal conductivity dependence on the dislocation line density for two sets of material parameters and the impurity concentrations (see

TABLE II. Ionic radii and typical impurity profiles[c] in GaN.

Material	Ionic radius (pm)	A (cm^{-3})	B (cm^{-3})	C (cm^{-3})
Oxygen	140	1×10^{17}	6×10^{16}	3×10^{16}
Hydrogen	208	2×10^{17}	3×10^{17}	1.4×10^{20}
Silicon	41	3×10^{16}	1.5×10^{17}	1.4×10^{20}
Carbon	260	3×10^{16}	6×10^{15}	2×10^{17}

[c]From Ref. 25.

Downloaded 19 Aug 2002 to 138.23.167.22. Redistribution subject to AIP license or copyright, see http://ojps.aip.org/japo/japcr.jsp

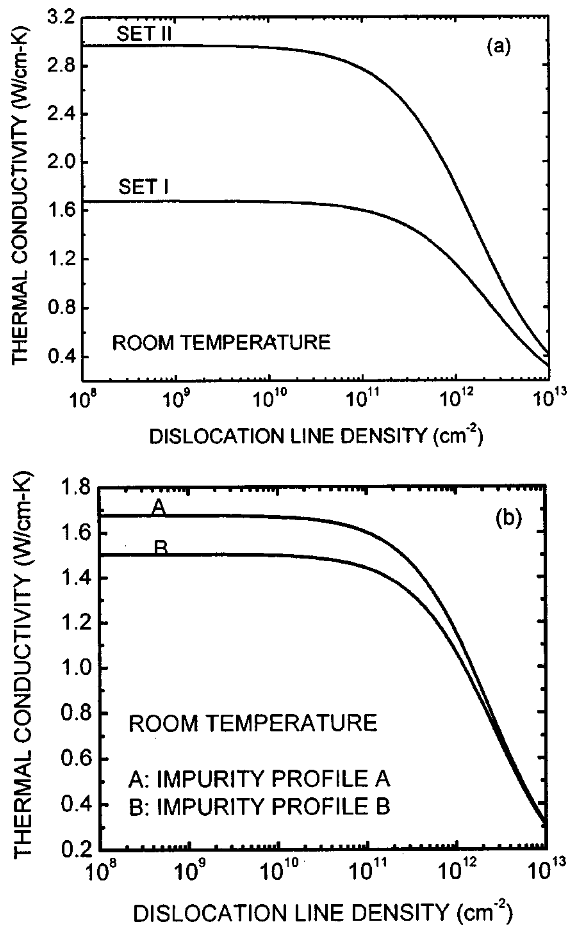

FIG. 2. Room-temperature thermal conductivity of wurtzite GaN films as a function of dislocation line density calculated for (a) two sets of material parameters and one fixed characteristic impurity profile; (b) one fixed set of material parameters and two different impurity profiles. One can see that at low dislocation density ($N_D < 10^{10}$ cm^{-2}) the thermal conductivity becomes independent of N_D and is defined by crystal anharmonicity and point-defect scattering.

Tables I and II). Different values of material parameters for GaN and impurity profiles used lead to the different thermal conductivity values at low dislocation density ($N_D = 10^8$ cm^{-2}). Figure 2(a) shows thermal conductivity for the same impurity profile but different material constants (Set I and Set II). Figure 2(b) demonstrates two thermal conductivity curves for exactly the same material parameters (Set I) but different impurity profiles (columns A and B of Table II). Despite ambiguity in material constants and a range of obtained thermal conductivity values that span from 1.51 to 2.95 W/cm K at low dislocation density, the obtained results are quite realistic and in line with reported experimental data.[5–7] As the dislocation density exceeds $N_D = 10^{10}$ cm^{-2} the thermal conductivity starts to decrease. In the range $N_D = 10^{10}$– 10^{12} cm^{-2} one can observe strong dependence of the room-temperature thermal conductivity on the dislocation line density. This result is in agreement with experimental data for LEO samples characterized by over a two-order-of-magnitude difference in dislocation density between the stripe and seam regions.[5] For low dislocation density ($N_D < 10^{10}$ cm^{-2}) the room-temperature thermal conductivity does not depend on N_D and is determined by intrinsic prop-

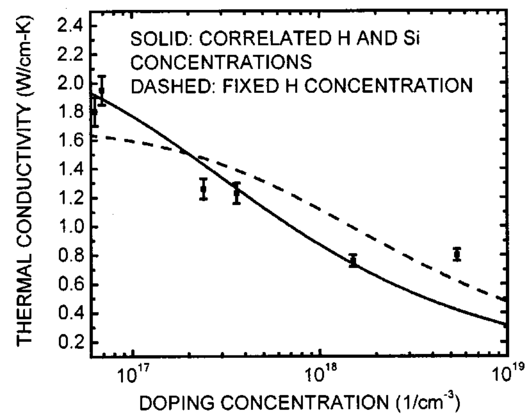

FIG. 3. Thermal conductivity in Si-doped GaN films as a function of doping concentration. The solid curve corresponds to the case when an increase in silicon doping density n_{Si} is accompanied by the increase in the hydrogen n_H impurity concentration. The dashed curve corresponds to the case when the hydrogen impurity concentration is a fixed value $n_H = 2\times 10^{17}$ cm^{-3}, and only silicon doping density n_{Si} changes. Note that an order of magnitude increase in the doping density (carrier concentration) leads to about a factor of 2 decrease in the thermal conductivity: specifically, from 1.77 to 0.86 W/cm K for the solid curve. Experimental points indicated with error bars are taken from Ref. 6.

erties, e.g., Umklapp scattering, and point defects.

Florescu *et al.*[6] experimentally determined that thermal conductivity decreases linearly with $\log(n)$, the variation being about a factor of 2 decrease in κ for every decade increase in the carrier concentration n. Here we examine this dependence theoretically on the basis of the model described above. For simplicity we neglect the scattering of acoustic phonons on electrons.[18] It is known that the free carrier scattering contribution to thermal resistance is small compared to that of static imperfections.[11] We assume that measured decrease in κ is due to increased phonon scattering on impurities whose density changes with increasing doping level. The electron density n in n-GaN films is correlated with the concentration of silicon dopants n_{Si}. Thus, one has to calculate thermal conductivity as a function of the doping density. Here two cases need to be considered. First, the concentration of Si dopants n_{Si} is an independent parameter, and one can change n_{Si} while keeping other impurity concentrations fixed. Second, the concentration of Si dopants is correlated with the hydrogen impurity concentration n_H. Changing n_{Si} in the point-defect scattering term, we should also change n_H. The former case allows us to elucidate the mechanism of the decrease easier while the latter seems to be more realistic according to experimental reports.[25] In Ref. 25 an increase in the concentration of H due to increase in Si doping in n-type GaN (such that $n_{Si} \approx n_H$) has been described. It has been attributed to negative H^- ion attachment to positive ions of silicon at anti-bonding Ga sites.

Figure 3 shows thermal conductivity in Si-doped n-GaN at room temperature as a function of carrier concentration n, which is assumed to be equal to the concentration of silicon dopants. The dashed curve corresponds to changing n_{Si} $(=n)$ and fixed n_H, while the solid curve corresponds to $n_{Si} \approx n_H$. Typical experimental points from Ref. 6 are indicated with error bars. As one can see in both cases, the theoretical curves closely follow the $\log(n)$ dependence. An order of

Downloaded 19 Aug 2002 to 138.23.167.22. Redistribution subject to AIP license or copyright, see http://ojps.aip.org/japo/japcr.jsp

magnitude increase in the carrier concentration (from 10^{17} to 10^{18} cm^{-3}) leads to about a factor of 2 decrease in the thermal conductivity, from 1.77 to 0.86 W/cm K. Our calculated dependence agrees well with indicated experimental results from Ref. 6. The theoretical curves intersect at $n_{Si}=n_H=2\times10^{17}$ cm^{-3}, a point where impurity scattering terms become identical. On the basis of our calculations we can conclude that the decrease of the thermal conductivity with increasing carrier concentration is mostly due to increase in phonon scattering on silicon dopants and, possibly, accompanying hydrogen impurities. Some deviation of theoretical curves from experimental results can be due to ambiguity of material parameters for GaN and omission of the acoustic phonon–electron scattering. The latter is reserved for future study. The boundary scattering and phonon spectrum modification,[28,29] which become significant in ultrathin films (quantum wells) were not included either since the film thickness was assumed to be much larger than the phonon mean-free path.

IV. CONCLUSION

We have calculated the lattice thermal conductivity in wurtzite GaN films as the function of doping density and defect concentrations. The performed calculation is material specific and includes thermal resistance due to impurities (O, H, Si, C) and dislocations (edge, screw, mixed) characteristic for GaN films. It is found that the intrinsic thermal conductivity, e.g., theoretical limit due to crystal anharmonicity, in wurtzite GaN is rather high $\kappa=3.36-5.40$ W/cm K. The range of values is a manifestation of difference in materials parameters reported for GaN in literature. We have also shown that the experimentally observed linear decrease of the thermal conductivity with logarithm of the carrier concentration can be explained by strongly enhanced phonon relaxation on Si dopants. Our calculations show that the increase in the doping density from 10^{17} to 10^{18} cm^{-3} leads to about a factor of 2 decrease in the thermal conductivity from 1.77 to 0.86 W/cm K. We have also established that the room-temperature thermal conductivity in GaN can be limited by dislocations when their density is high, e.g., $N_D>10^{10}$ cm^{-2}. The results of our calculations are in good agreement with the experimental data.

ACKNOWLEDGMENTS

The work in UCR was supported in part by ONR Young Investigator Award No. N000140210352 and NSF Faculty Early CAREER Development Award No. ECS-0093959 to A. B. The work of D. I. F. and F. H. P. was supported by ONR Contract No. N00014-99-C-0663, administered by Dr. Colin Wood.

[1] R. Gaska, A. Osinsky, J. W. Yang, and M. S. Shur, IEEE Electron Device Lett. **19**, 89 (1998).
[2] L. F. Eastman, V. Tilak, J. Smart, B. M. Green, E. M. Chumbes, R. Dimitrov, Kim Hyungtak, O. S. Ambacher, N. Weimann, T. Prunty, M. Murphy, W. J. Schaff, and J. R. Shealy, IEEE Trans. Electron Devices **48**, 479 (2001).
[3] R. Dietrich, A. Wieszt, A. Vescan, and H. Leier, in Proceedings of the 4th International Conference On Nitride Semiconductors, 2001, Denver, CO.
[4] E. K. Sichel and J. I. Pankove, J. Phys. Chem. Solids **38**, 330 (1997).
[5] D. I. Florescu, V. M. Asnin, and F. H. Pollak, A. M. Jones, J. C. Ramer, M. J. Schurman, and I. Ferguson, Appl. Phys. Lett. **77**, 1464 (2000); D. I. Florescu, V. M. Asnin, and F. H. Pollak, Compound Semicond. **7**, 62 (2001).
[6] D. I. Florescu, V. M. Asnin, F. H. Pollak, R. J. Molnar, and C. E. C. Wood, J. Appl. Phys. **88**, 3295 (2000).
[7] C.-Y. Luo, H. Marchand, D. R. Clarke, and S. P. DenBaars, Appl. Phys. Lett. **75**, 4151 (1999).
[8] D. Kotchetkov, J. Zou, A. A. Balandin, D. I. Florescu, and F. H. Pollak, Appl. Phys. Lett. **79**, 4316 (2001).
[9] C. J. Glassbrenner and G. A. Slack, Phys. Rev. **134**, A1058 (1964); E. Yamasue, M. Susa, H. Fukuyama, and K. Nagata, J. Cryst. Growth **234**, 121 (2002).
[10] J. Callaway, Phys. Rev. **113**, 1046 (1959).
[11] P. G. Klemens, in *Solid State Physics*, edited by F. Seitz and D. Turnbull (Academic, New York, 1958), Vol. 7.
[12] S. Nakamura, S. Pearton, and G. Fasol, in *The Blue Laser Diode: The Complete Story* (Springer, Berlin, 2000); V. Bougrov, M. Levinshtein, S. L. Rumyantsev, and A. Zubrilov, *Properties of Advanced Semiconductor Materials*, edited by M. E. Levinshtein, S. L. Rumyantsev, M. S. Shur, (Wiley, New York, 2001); S. Strite, and H. Markoc J. Vac. Sci. Technol. B **10**, 1237 (1992).
[13] T. Deguchi, D. Ichiryu, K. Toshikawa, K. Sekiguchi, T. Sota, R. Matsuo, T. Azuhata, M. Yamaguchi, T. Yagi, S. Chichibu, and S. Nakamura, J. Appl. Phys. **86**, 1860 (1999).
[14] A. Polian, M. Grimsditch, and I. Grzegory, J. Appl. Phys. **79**, 3343 (1996).
[15] P. G. Klemens, in *Chem. and Phys. of Nanostructures and Related Non-Equilibrium Materials*, edited by E. Ma, B. Fultz, R. Shall, J. Morral, and P. Nash (Minerals, Metals, and Materials Society, Warrendale, PA, 1997), p. 97.
[16] K. Karch, J.-M. Wagner, and F. Bechstedt, Phys. Rev. B **57**, 7043 (1998).
[17] P. G. Klemens, Proc. Phys. Soc. LXVIII **12-A**, 1113 (1955).
[18] C. M. Bhandari and D. M. Rowe, in *Thermal Conduction in Semiconductors* (Wiley, New York, 1988).
[19] A. F. Wright and Ulrike Grossner, Appl. Phys. Lett. **73**, 2751 (1998).
[20] M. Albrecht, I. P. Nikitina, A. E. Nikolaev, Yu. V. Melnik, V. A. Dmitriev, and H. P. Strunk, Phys. Status Solidi A **176**, 453 (1999).
[21] J. Elsner, R. Jones, and P. K. Sitch, V. D. Porezag, M. Elstner, Th. Frauenheim, M. I. Heggie, S. Oberg, and P. R. Briddon, Phys. Rev. Lett. **79**, 3672 (1997).
[22] G. A. Slack, J. Phys. Chem. Solids **34**, 321 (1973).
[23] A. Witek, Diamond Relat. Mater. **7**, 962 (1998).
[24] R. B. Schwarz, K. Khachataryan, and E. R. Weber, Appl. Phys. Lett. **70**, 1122 (1997).
[25] S. J. Pearton, J. C. Zolper, R. J. Shul, and F. Ren, J. Appl. Phys. **86**, 1 (1999).
[26] R. Zhang and T. F. Kuech, Appl. Phys. Lett. **72**, 1611 (1998).
[27] J. Neugebauer and C. G. Van de Walle, Appl. Phys. Lett. **69**, 503 (1996).
[28] A. Balandin and K. L. Wang, Phys. Rev. B **58**, 1544 (1998).
[29] J. Zou and A. Balandin, J. Appl. Phys. **89**, 2932 (2001).

Downloaded 19 Aug 2002 to 138.23.167.22. Redistribution subject to AIP license or copyright, see http://ojps.aip.org/japo/japcr.jsp